From Extension of Loop's Approximation Scheme to Interpolatory Subdivisions

Charles K. Chui[1], Qingtang Jiang[2]
Department of Mathematics and Computer Science
University of Missouri–St. Louis
St. Louis, MO 63121, U.S.A.

Abstract

The minimum-supported bivariate C^2-cubic spline on a 6-directional mesh constructed in our previous work [2] can be used to extend Loop's approximation subdivision scheme to introduce some parameter for controlling surface geometric shapes. This extension is achieved by considering matrix-valued subdivisions, resulting in subdivision templates of the same 1-ring template size as Loop's scheme, but with 2-dimensional matrix-valued weights. Another feature accomplished by considering such an extension is that the two components of the refinable vector-valued spline function can be reformulated, by taking certain linear combinations, to convert the approximation scheme to an interpolatory scheme, but at the expense of an increase in template size for the edge vertices. To maintain the 1-ring template size with guarantee of C^2 smoothness for interpolatory surface subdivisions, a non-spline solution is needed, by applying some constructive scheme such as the procedure discussed in our recent work [4]. The main objective of this paper is to develop the corresponding matrix-valued 1-ring templates for the extraordinary vertices of arbitrary valences, for all of the three schemes mentioned above: the extended Loop approximation scheme, its conversion to an interpolatory scheme, and the non-spline 1-ring interpolatory scheme. The discrete Fourier transform (DFT) is applied to analyze the spectral properties of the corresponding subdivision matrices, assuring that the eigenvalues of the subdivision matrices satisfy certain conditions for C^1 smoothness at the extraordinary vertices for all of the three considerations in this paper.

1. Introduction

Subdivision algorithms provide efficient mathematical tools for curve and surface modelling, rendering, and editing in Computer Graphics (see, for example, [21, 18]). To construct a smooth surface, the subdivision process is carried out iteratively, starting from an initial (triangular or quadrilateral) mesh, called control net, to generate some nested sequence of finer and finer meshes that eventually converge to the desirable limiting surface, called subdivision surface. If all the vertices of each coarser mesh (i.e. the mesh before the next iteration step is carried out) are among the vertices of the finer mesh (i.e. the mesh obtained after the next iteration step has been completed), then the subdivision scheme is called an *interpolatory subdivision scheme*. Otherwise, it is called an *approximation subdivision scheme*.

[1]Research supported by ARO Grant #W911NF-04-1-0298 and DARPA/NGA Grant #HM1582-05-2-0003. This author is also with the Department of Statistics, Stanford University, Stanford, CA 94305.
[2]Research supported by UM Research Board 10/05 and UMSL Research Award 10/06.

For surface subdivisions, this iterative process is governed by two sets of rules, namely: the *topological rule* that dictates the insertion of new vertices and the connection of them to create a finer mesh, and the *local averaging rule* for computing the positions in the 3-dimensional space $\mathbb{R}^3$ of the new vertices (and for an approximation subdivision scheme, new positions of the old ones as well) in terms of certain weighted averages of the (old) vertices nearby. The most popular topological rule for surface subdivisions is the "1-to-4 split" (or dyadic) rule, which dictates the split of each triangle or quadrilateral into four triangles or quadrilaterals, respectively. For example, the Catmull-Clark [1], Doo-Sabin [7], Loop [12], butterfly [8], and mid-edge [13] schemes, are the most well-known schemes that engage the 1-to-4 split topological rule.

For regular vertices (i.e. those with valence 6 for triangular subdivisions, and valence 4 for quadrilateral subdivisions), the local averaging rule of the iterative process for the 1-to-4 split topological rule is related to some refinement equation

$$\phi(\mathbf{x}) = \sum_{\mathbf{k}\in\mathbf{Z}^2} p_{\mathbf{k}}\phi(2\mathbf{x}-\mathbf{k}), \quad \mathbf{x}\in\mathbb{R}^2. \tag{1.1}$$

Here, $\phi(\mathbf{x})$ is called a refinable function with dilation matrix $2I_2$, and the (finite) sequence $\{p_{\mathbf{k}}\}$ is called its corresponding refinement sequence or subdivision mask. For a control net with vertices $v^0_{\mathbf{k}}$, called "control points", the subdivision mask $\{p_{\mathbf{k}}\}$ provides the local averaging rule

$$v^{m+1}_{\mathbf{j}} = \sum_{\mathbf{k}} v^m_{\mathbf{k}} p_{\mathbf{j}-2\mathbf{k}}, \quad m = 0, 1, \cdots, \tag{1.2}$$

where, for each $m = 1, 2, \cdots$, the set $v^m_{\mathbf{k}}$ denotes the set of vertices obtained after taking m iterations. The local averaging rule (1.2) is, in general, described and represented in the plane, called the "parametric domain", by a set of regular triangles or quadrilaterals along with a set of subdivision templates. For example, for Loop's scheme, where the refinable function ϕ is the quartic box spline B_{222} on a 3-directional mesh, the templates of its local averaging rule for the 1-to-4 split triangular mesh are shown on the left and in middle among the three templates in Fig.1. On the other hand, to take care of ex-

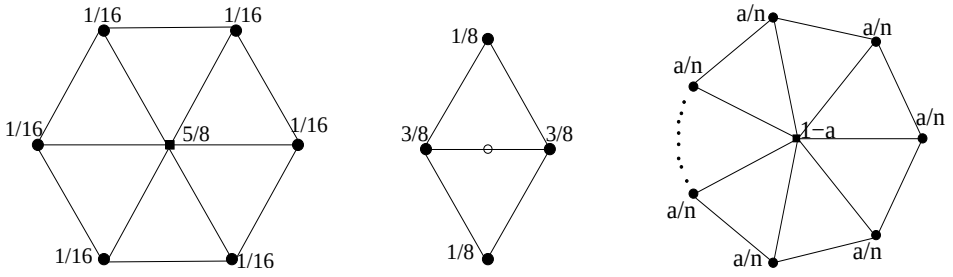

Figure 1: *Templates of Loop's scheme for regular vertices, edge vertices, and extraordinary vertices with valence n, where* $a = \frac{5}{8} - (\frac{3}{8} + \frac{1}{4}\cos\frac{2\pi}{n})^2$

traordinary vertices (i.e. those with valences different from 6 for triangular subdivisions, and valences different from 4 for quadrilateral subdivisions), a certain custom-designed

local averaging rule is required in general. For example, the template for Loop's scheme for extraordinary vertices of valence n is shown on the right among the three templates in Fig.1, where

$$a = \frac{5}{8} - (\frac{3}{8} + \frac{1}{4}\cos\frac{2\pi}{n})^2 \tag{1.3}$$

is a function of the valence n. Consequently, smoothness of subdivision surfaces at extraordinary vertices is not determined by that of ϕ. The interested reader is referred to [16] and the references therein for detailed discussions on smoothness analysis at extraordinary vertices, and to [11] and the references therein for estimates of order of smoothness for non-spline refinable functions ϕ.

In another development, namely, that of multi-wavelets in Wavelet Analysis, the refinement equation (1.1) is extended to a matrix-valued refinement (also called two-scale) relation

$$\Phi(\mathbf{x}) = \sum_{\mathbf{k}\in\mathbf{Z}^2} P_{\mathbf{k}}\Phi(A\mathbf{x} - \mathbf{k}), \quad \mathbf{x} \in \mathbb{R}^2, \tag{1.4}$$

with dilation matrix A (which could be the matrix $2I_2$ in (1.1)), an r-dimensional vector-valued refinable function $\Phi = [\phi_0, \cdots, \phi_{r-1}]^T$ (also called refinable function vector), and refinement (or two-scale) sequence of r-dimensional square matrices $\{P_{\mathbf{k}}\}$, which will be called a subdivision mask in this paper.

For the 1-to-4 split topological rule, we just select $2I_2$ as the dilation matrix A. But for other topological rules, such as $\sqrt{2}$, $\sqrt{3}$, $\sqrt{5}$ and $\sqrt{7}$ splits, different appropriate dilation matrices must be chosen. For example, in the study of $\sqrt{3}$-subdivisions, the dilation matrix

$$A_1 = \begin{bmatrix} 2 & -1 \\ 1 & -2 \end{bmatrix} \tag{1.5}$$

is used in our earlier paper [2] to construct a 2-dimensional refinable function vector with bivariate C^2 cubic spline components on a 6-directional mesh. It was also observed in [2] that this particular spline function vector is also refinable with respect to the dilation matrix $2I_2$; and hence, the corresponding subdivision mask provides another set of templates for generating subdivision surfaces for the 1-to-4 split topological rule, but with (2-dimensional) matrix-valued weights, instead of scalar-valued weights. For convenience, we will refer to this matrix-valued subdivision scheme as "S_3^2-subdivision". The matrix-valued weights of the S_3^2-subdivision provide a free parameter (called control parameter in [2]), for adjusting shapes of surface geometry. In particular, when the control parameters are set to be zero at each iterative step, then the subdivision surface generated by S_3^2-subdivision is identical to the subdivision surface generated by Loop's scheme. For this reason, S_3^2-subdivision can be considered as an extension of Loop's scheme. In this paper, subdivision templates with sizes not exceeding those of Loop's scheme will be called "1-ring" templates.

Most surface subdivision schemes in the existing literature, including Loop's scheme and its extension to S_3^2-subdivision, are not interpolatory, meaning that the control points (or vertices of the initial mesh) do not lie on the (limiting) subdivision surface. In certain applications, such as reversed engineering of scattered data and study of

point clouds, where control points are data points, surface interpolation is an important requirement. For matrix-valued subdivisions, various versions of interpolatory subdivisions were introduced, particularly for the purpose of Hermite interpolation (see, for example, [9, 2, 3, 6]). These considerations, however, are too restrictive to be useful for the construction of interpolatory matrix-valued templates in general, particularly when symmetry is an essential feature. The most general extension of interpolatory surface subdivisions, from scalar to matrix considerations and without any restriction, for constructing symmetric interpolatory matrix-valued templates is formulated in our earlier paper [4].

The characterization of interpolatory subdivision matrices derived in [4] can be easily applied to convert the S_3^2-subdivision to interpolatory surface subdivisions, which will be called "S_3^2-interpolatory-subdivision" in this paper. Hence, extending Loop's scheme, by allowing matrix-valued weights to replace scalar-valued weights, has the flexibility to achieve spline-based surface interpolation of the control points, which are vertices of the initial control net.

Unfortunately, this spline approach necessarily increases the template size for edge vertices (if the weights are required to remain 2-dimensional matrices). In order to maintain 1-ring templates as well as not to increase the matrix dimension, while achieving C^2 interpolatory subdivision, a non-spline solution was obtained in [4]. It will be called "1-ring-interpolatory-subdivision" in this paper. However, the above discussions of S_3^2-subdivision, S_3^2-interpolatory-subdivision, and 1-ring-interpolatory-subdivision so far are only concerned with regular vertices.

The main objective of this paper is to derive 1-ring templates for extraordinary vertices, with arbitrary valences, for all of these three surface subdivision schemes. After giving a brief introduction to the prior work on the matrix-valued subdivision in Section 2, we present the results on templates for extraordinary vertices in Sections 3, 4, and 5 for S_3^2-subdivision, S_3^2-interpolatory-subdivision, and 1-ring-interpolatory-subdivision, respectively. Spectral analysis of the subdivisions matrices by using the discrete Fourier transform (DFT), as well as discussions on the choice of control parameters for the 1-ring-interpolatory-subdivision scheme, will be presented in the appendix.

To facilitate our discussions, let us first introduce the following notations. We will use $\mathbf{0}$ to denote the zero matrix of any dimension, but specifically use 0_j and $0_{j\times k}$ to denote the $j \times j$ and $j \times k$ zero matrices, respectively. Eigenvalues $\lambda_j, j = 0, 1, \cdots$, of a subdivision matrix are always listed according to multiplicities and indexed in the order of non-increasing magnitudes, namely:

$$|\lambda_0| \geq |\lambda_1| \geq |\lambda_2| \geq \cdots,$$

with the second and third eigenvalues λ_1, λ_2 to be called subdominant eigenvalues.

2. Prior results

When the matrix-valued refinement equation (1.4) is applied to surface subdivisions, the local averaging rule (1.2) is extended to the matrix setting:

$$\mathbf{v}_{\mathbf{k}}^{m+1} = \sum_{\mathbf{j}} \mathbf{v}_{\mathbf{j}}^{m} P_{\mathbf{k}-A\mathbf{j}}, \quad m = 0, 1, \cdots, \tag{2.1}$$

where

$$\mathbf{v}_{\mathbf{k}}^{m} =: [v_{\mathbf{k}}^{m}, s_{\mathbf{k},1}^{m} \cdots, s_{\mathbf{k},r-1}^{m}] \tag{2.2}$$

are "row-vectors" with r components of points $v_{\mathbf{k}}^{m}, s_{\mathbf{k},i}^{m}$, $i = 1, \cdots, r-1$, in $\mathbb{R}^3$. Here, we use the first components $v_{\mathbf{k}}^{m}$ to denote the vertices of the subdivision meshes generated after the m^{th} iteration, with initial vertices $v_{\mathbf{k}}^{0}$ being the control points of the surface subdivision. The other components $s_{\mathbf{k},1}^{0}, \cdots, s_{\mathbf{k},n-1}^{0}$ of $\mathbf{v}_{\mathbf{k}}^{0}$, can be used to control the surface geometric shape. Then, as shown in our earlier work [5], under the condition of "generalized partition of unity", the vertices $v_{\mathbf{k}}^{m}$ provide an accurate discrete approximation of the target subdivision surface, formulated by the series representation:

$$F(\mathbf{x}) = \sum_{\mathbf{k}} v_{\mathbf{k}}^{0} \phi_0(\mathbf{x} - \mathbf{k}) + \sum_{\mathbf{k}} \Big(s_{\mathbf{k},1}^{0} \phi_1(\mathbf{x} - \mathbf{k}) + \cdots + s_{\mathbf{k},n-1}^{0} \phi_{n-1}(\mathbf{x} - \mathbf{k}) \Big).$$

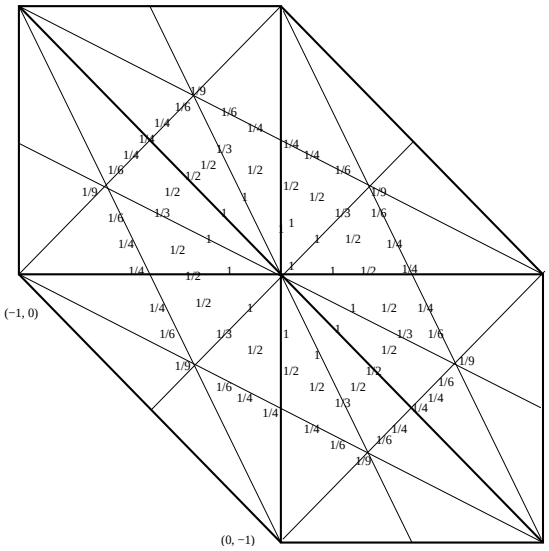

Figure 2: *Support and Bézier-nets of* ϕ_0^b

The bivariate C^2 cubic spline function ϕ_0^b with minimum support introduced in our earlier work [2] is shown in Fig.2, where only the nonzero Bézier coefficients are displayed. (Actually, $\phi_0^b(-x, y)$ is introduced in [2]. The reason for the choice of this ϕ_0^b here and in [5], as opposed to $\phi_0^b(-x, y)$ in [2], is to use the same domain of the characteristic map as that considered in [17].) By introducing another cubic spline

$$\phi_1^b(\mathbf{x}) := \phi_0^b((A_1^{-1})^T \mathbf{x}), \tag{2.3}$$

with A_1 given in (1.5), it is shown in [2] that the function vector $\Phi^b = [\phi_0^b, \phi_1^b]^T$ is refinable with respect to both dilation matrices $2I_2$ and A_1^T, with corresponding refinement masks that give rise to 1-to-4 split scheme (referred as S_3^2-subdivision) and $\sqrt{3}$ subdivision scheme, respectively. The interested reader is referred to [2] for details. On the other hand, for the 2-dimensional matrix-valued weights of the S_3^2-subdivision (which has a free control parameter), it was demonstrated in [5] that the control parameter could be applied to change the geometric shapes of subdivision surfaces quite dramatically.

Other matrix-valued templates with minimal size have also been constructed in our previous work [2, 3, 6] for different purposes. More precisely, [2] also presents C^1 Hermite interpolatory schemes both for 1-to-4 split and $\sqrt{3}$ split based on C^1 quadratic Hermite splines; [3] obtains a second-order Hermite basis of the space of C^2-quartic splines on a six-dimensional mesh to yield matrix-valued templates for Hermite interpolatory surface subdivision scheme for the 1-to-4 split triangular topological rule; [6] constructs refinable quartic and quintic spline function vectors on the four-directional mesh to generate matrix-valued templates for approximation and Hermite interpolatory surface subdivision schemes, respectively, for both the $\sqrt{2}$ and 1-to-4 split quadrilateral topological rules.

However, Hermite interploatory schemes lack the desirable symmetry, and they are too restrictive to be useful when the templates for extraordinary vertices are considered. A natural extension of interpolatory surface subdivisions from scalar to matrix considerations is introduced in [4]. More precisely, a subdivision scheme with matrix-valued templates, generated by some subdivision mask $\{P_{\mathbf{k}}\}$ corresponding to $2I_2$ dilation, is called interpolatory in [4], if $v_{2\mathbf{k}}^{m+1} = v_{\mathbf{k}}^m$, for all $m = 0, 1, \cdots, \mathbf{k} \in \mathbb{Z}^2$, where $v_{2\mathbf{k}}^{m+1}$ and $v_{\mathbf{k}}^m$ are the first components of $\mathbf{v}_{2\mathbf{k}}^{m+1}$ and $\mathbf{v}_{\mathbf{k}}^m$, respectively, and $\mathbf{v}_{\mathbf{k}}^m$ are defined as in (2.1). When we use the first components $v_{\mathbf{k}}^m$ to denote the vertices of the subdivision meshes generated after the m^{th} iteration, this definition precisely assures that the control points lie on the (limiting) subdivision surface, as in the scalar-valued setting. It is also shown in [4] that the algebraic structure of the interpolatory mask $\{P_{\mathbf{k}}\}$ is given by

$$P_{0,0} = \begin{bmatrix} 1 & * & \cdots & * \\ 0 & * & \cdots & * \\ \vdots & \vdots & \cdots & \vdots \\ 0 & * & \cdots & * \end{bmatrix}, \quad P_{2\mathbf{j}} = \begin{bmatrix} 0 & * & \cdots & * \\ \vdots & \vdots & \cdots & \vdots \\ 0 & * & \cdots & * \end{bmatrix}, \quad \mathbf{j} \in \mathbb{Z}^2 \backslash \{(0,0)\}. \tag{2.4}$$

We remark that when the matrix dimension r is 1, this property is reduced to the simple algebraic property

$$p_{2\mathbf{j}} = \delta(\mathbf{j}), \quad \mathbf{j} \in \mathbb{Z}^2, \tag{2.5}$$

of an interpolatory mask $\{p_{\mathbf{k}}\}$ for the scalar-valued setting, where as usual, we use $\delta(\mathbf{j})$ for the Kronecker delta symbol. It was also shown in [4] that under certain mild conditions that include the generalized partition of unity, the algebraic structure in (2.4) is equivalent to the following Lagrange-type interpolation property of the refinable function vector $\Phi = [\phi_0, \phi_1, \cdots, \phi_{r-1}]^T$, namely:

$$\phi_0(\mathbf{k}) = \delta(\mathbf{k}), \quad \phi_j(\mathbf{k}) = 0, \quad \mathbf{k} \in \mathbb{Z}^2, \ 1 \le j \le r-1. \tag{2.6}$$

Let ϕ_0^b be the minimum support bivariate C^2 cubic spline shown in Fig.2, and ϕ_1^b be the spline defined by (2.3). Since $\phi_1^b(0,0) = 1 \neq 0$, and

$$\begin{aligned}&\phi_1^b(\cdot-(1,0)) = \phi_1^b(\cdot-(-1,1)) = \phi_1^b(\cdot-(0,1))\\ &= \phi_1^b(\cdot+(1,0)) = \phi_1^b(\cdot+(-1,1)) = \phi_1^b(\cdot+(0,1)) = \frac{1}{9} \neq 0,\end{aligned}$$

it follows that the masks corresponding to the refinable function vectors $[c_0\phi_0^b+c_1\phi_1^b, c_2\phi_0^b+c_3\phi_1^b]$ are not interpolatory for all choices of c_j, with $c_0c_3 - c_1c_2 \neq 0$. However, as in [4], by introducing

$$\begin{aligned}\widetilde{\phi}_1^b := \phi_1^b - \phi_0^b - \frac{1}{9}\{&\phi_0^b(\cdot-(1,0)) + \phi_0^b(\cdot-(-1,1)) + \phi_0^b(\cdot-(0,1))\\ &+ \phi_0^b(\cdot+(1,0)) + \phi_0^b(\cdot+(-1,1)) + \phi_0^b(\cdot+(0,1))\},\end{aligned}$$

so that $\phi_0^b, \widetilde{\phi}_1^b$ satisfy (2.6) (with ϕ_0, ϕ_1 replaced by $\phi_0^b, \widetilde{\phi}_1^b$, respectively). It is easy to verify that $[\phi_0^b,\ \widetilde{\phi}_1^b]^T$ is also refinable with respect to the dilation matrices $2I_2$, so that its refinement mask gives rise to an interpolatory scheme.

In [4], except this spline-based C^2 interpolatory scheme, various matrix-valued spline-based and non-spline-based interpolatory schemes for $\sqrt{3}$, $\sqrt{2}$ subdivisions and 1-to-4 split triangular and quadrilateral subdivisions are constructed.

3. C^2 cubic spline-based approximation schemes

This section is devoted to the construction of 1-ring templates for extraordinary vertices for the S_3^2-subdivision. In this paper, we only consider the 1-to-4 split topological rule, and will use $\{P_{\mathbf{k}}^b\}$ to denote the refinement mask of $\Phi^b = [\phi_0^b, \phi_1^b]^T$ corresponding to the dilation matrix $2I_2$. Observe that for any non-singular 2×2 constant matrix U, the function vector $U\Phi^b$ is also refinable with respect to the dilation matrix $2I_2$, with corresponding refinement mask given by $\{UP_{\mathbf{k}}^bU^{-1}\}$. We are particularly interested in the choice of

$$U = \begin{bmatrix} \frac{1}{3} & 1 \\ -\frac{1}{3} & 1 \end{bmatrix},$$

since the subdivision scheme for this choice provides a matrix extension of Loop's scheme, with some free control (or shape-control) parameter. More precisely, let $\Phi = U[\phi_0^b,\ \phi_1^b]^T$, namely:

$$\Phi := [\frac{1}{3}\phi_0^b + \phi_1^b, -\frac{1}{3}\phi_0^b + \phi_1^b]^T. \tag{3.1}$$

Then the nonzero matrices of its subdivision mask $\{P_{\mathbf{k}}\}$ are given by

$$\begin{aligned}&P_{0,0} = \begin{bmatrix} \frac{5}{8} & \frac{3}{8} \\ \frac{3}{8} & -\frac{1}{8} \end{bmatrix}, \qquad (3.2)\\ &P_{1,0} = P_{-1,0} = P_{0,1} = P_{0,-1} = P_{1,1} = P_{-1,-1} = X,\\ &P_{2,1} = P_{-2,-1} = P_{1,2} = P_{-1,-2} = P_{1,-1} = P_{-1,1} = Y,\\ &P_{2,0} = P_{-2,0} = P_{0,2} = P_{0,-2} = P_{2,2} = P_{-2,-2} = Z,\end{aligned}$$

where

$$X = \begin{bmatrix} \frac{3}{8} & 0 \\ \frac{1}{4} & \frac{1}{8} \end{bmatrix}, \quad Y = \begin{bmatrix} \frac{1}{8} & 0 \\ \frac{1}{8} & 0 \end{bmatrix}, \quad Z = \begin{bmatrix} \frac{1}{16} & -\frac{1}{16} \\ \frac{1}{16} & -\frac{1}{16} \end{bmatrix}. \tag{3.3}$$

The templates for the local averaging rule derived from this subdivision mask are shown on the left and in middle among the three templates in Fig.3. In this case, the constant vector $\mathbf{y}_0$ for which Φ reproduces all non-zero constants is given by $\mathbf{y}_0 = [1, 0]$. This means that $\mathbf{y}_0 = [1, 0]$ is the desirable constant vector for which

$$\mathbf{y}_0 \sum_{\mathbf{k} \in \mathbf{Z}^2} \Phi(\mathbf{x} - \mathbf{k}) = constant, \quad \mathbf{x} \in \mathbb{R}^2.$$

The interested reader is referred to [10] and the references therein for some detailed discussion of polynomial reproduction by Φ. This matrix-valued subdivision scheme with templates on the left and in middle of Fig.3 is still refereed as "S_3^2-subdivision".

In the following, we will introduce the corresponding templates for treating extraordinary vertices such that the S_3^2-subdivision scheme will assure the eigenvalues λ_j of the subdivision matrix satisfying $\lambda_0 = 1, \lambda_1 = \lambda_2, |\lambda_3| < |\lambda_1|$.

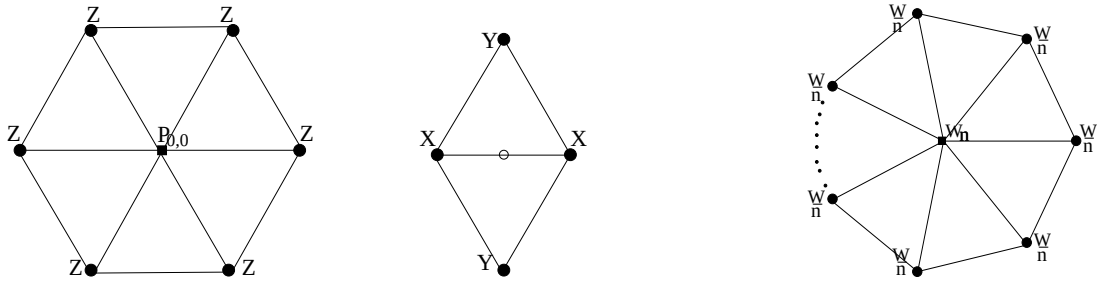

Figure 3: *Templates for S_3^2-subdivision for regular vertices (left and middle), and for extraordinary vertices with valence n (right)*

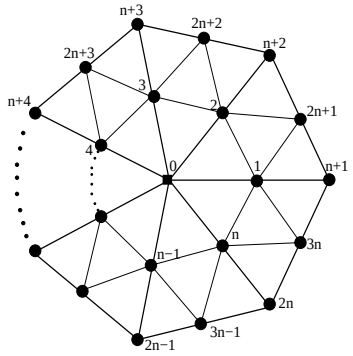

Figure 4: *Labeling of the indices*

For extraordinary vertices with valence n, we will determine the 2×2 matrices W_n and W (both depending on n) for the 1-ring template as shown on the right in Fig.3. To construct these matrices, we need to analyze the spectral property of the subdivision

matrix. Here, an appropriate labeling of the indices of the vertices is important, and we will follow [19]. Although we need to start with a 3-ring template, it is sufficient to illustrate the order of the indices by only considering a 2-ring neighborhood of an extraordinary vertex with valence n, as shown in Fig.4. To analyze the surface smoothness for 1-ring templates, we first consider a subdivision matrix, denoted by S_P, on a 3-ring neighborhood of the extraordinary vertex of valence n. By applying some appropriate permutations to the DFT of S_P, we arrive at a block diagonal matrix (see the first appendix for the derivation), with n diagonal blocks

$$M_0 = \begin{bmatrix} m_0 & * \\ 0_{6\times 8} & 0_6 \end{bmatrix}, \qquad M_j = \begin{bmatrix} m_1(z^j) & * \\ 0_6 & 0_6 \end{bmatrix}, \quad 1 \le j \le n-1, \tag{3.4}$$

where

$$z := e^{i\frac{2\pi}{n}}, \tag{3.5}$$

and

$$m_0 = \begin{bmatrix} W_n & X & Z & Y \\ W & X+2Y & P_{0,0}+2Z & 2X \\ 0 & 0 & Z & 0 \\ 0 & 0 & 2Z & Y \end{bmatrix},$$

$$m_1(z) = \begin{bmatrix} X+Y(z+\frac{1}{z}) & P_{0,0}+Z(z+\frac{1}{z}) & X(1+z) \\ 0 & Z & 0 \\ 0 & Z(1+\frac{1}{z}) & Y \end{bmatrix}.$$

Here, Z only has zero eigenvalues, Y has one non-zero eigenvalue $\frac{1}{8}$, and

$$X + Y(z^j + \frac{1}{z^j}) = \begin{bmatrix} \frac{3}{8} + \frac{1}{4}\cos\frac{2\pi j}{n} & 0 \\ \frac{1}{4}(1+\cos\frac{2\pi j}{n}) & \frac{1}{8} \end{bmatrix}.$$

Thus, the non-zero eigenvalues of S_P consist of those of the matrix

$$\begin{bmatrix} W_n & X \\ W & X+2Y \end{bmatrix}$$

as well as the values

$$\frac{1}{8} \text{ (with multiplicity } 2n-1), \quad \frac{3}{8} + \frac{1}{4}\cos\frac{2\pi j}{n}, \quad 1 \le j \le n-1.$$

Set

$$W = 16aZ = \begin{bmatrix} a & -a \\ a & -a \end{bmatrix}, \quad W_n = \begin{bmatrix} 1-a & a \\ x_3 & x_4 \end{bmatrix}, \tag{3.6}$$

where a is the weight used in Loop's scheme as shown in (1.3), and $x_3, x_4 \in \mathbb{R}$. For such W and W_n, the eigenvalues of $\begin{bmatrix} W_n & X \\ W & X+2Y \end{bmatrix}$ consist of the values $1, \frac{1}{8}$, and

$$\lambda_\pm = \frac{5}{16} + \frac{x_4 - a}{2} \pm \frac{1}{16}\sqrt{64a^2 - 176a + 128ax_4 + 25 - 80x_4 + 64x_4^2 + 256ax_3}.$$

Analogous to Loop's scheme, we set

$$\lambda_+ = (\frac{3}{8} + \frac{1}{4}\cos\frac{2\pi}{n})^2.$$

Then we have

$$x_3 = \frac{3}{8}, \quad x_4 = \lambda_-.$$

So, by choosing a sufficiently small value of λ_-, we can select appropriate values of $x_4(=\lambda_-)$. For example, we may set x_4 to be $0, \frac{1}{32}, \frac{1}{16}, \frac{1}{8}$ or $-\frac{1}{8}$, respectively. Here we would like to remark that for the particular choice of $x_4 = -\frac{1}{8}$, W_n and W with $n = 6$ are exactly the same as the weights $P_{0,0}$ and $6Z$ for regular vertices, as given in (3.2) and (3.3), respectively.

For valence $n = 4$, with the vertices of the octahedron shown on the top-left of Fig. 5 as the control net (or initial mesh), we apply S_3^2-subdivision. Since the second component of $\mathbf{y}_0 = [1, 0]$ for constant reproduction is 0, according to a preliminary study of the choice of control parameter in [5], we simply choose $\mathbf{0}$ as the control parameter. The resulting subdivision surfaces are shown on the top-right and bottom-left of Fig. 5 with $x_4 = -\frac{1}{8}$ and $x_4 = \frac{1}{16}$, respectively. In comparison with the limiting surface obtained by applying Loop's scheme (shown on the bottom-right of Fig.5), it is clear that the S_3^2-subdivision is the desirable choice, particularly for such applications as point-clouds visualization and reverse engineering, where the data points are used as control vertices.

As discussed above, the leading eigenvalues of the corresponding subdivision matrix S_P satisfy the conditions

$$\lambda_0 = 1, \quad \lambda_1 = \lambda_2, \quad |\lambda_3| < |\lambda_1|. \tag{3.7}$$

If the characteristic map for the matrix-valued subdivision is regular and injective, then the subdivision surface is C^1 near extraordinary vertices (see [15, 5]). One may study the regularity and injectivity of the characteristic map as in [5] by representing the partial derivatives of the characteristic map in terms of the Bézier-nets. In this regard, we remark that the regularity and injectivity of the characteristic maps, corresponding to the matrix-valued subdivision scheme based on ϕ_0^b, ϕ_1^b, have been verified for extraordinary vertices with valence 3 and 4 in [5]. See also [14, 17] for detailed discussions in the scalar setting. Here and in what follows, let us only retreat to visual judgement as discussed below.

Let $\mathbf{U}^1, \mathbf{U}^2$ be two real-valued (linearly independent) eigenvectors that correspond to the subdominant eigenvalues λ_1, λ_2. Note that $\mathbf{U}^1, \mathbf{U}^2$ are $2(6n+1)$-vectors, namely,

$$\mathbf{U}^1 = [u_1^1, u_2^1, \cdots, u_{2(6n+1)}^1], \quad \mathbf{U}^2 = [u_1^2, u_2^2, \cdots, u_{2(6n+1)}^2].$$

Write

$$\mathbf{U}^1 =: [\mathbf{u}_0^1, \cdots, \mathbf{u}_{6n}^1], \quad \mathbf{U}^2 =: [\mathbf{u}_0^2, \cdots, \mathbf{u}_{6n}^2],$$

where

$$\mathbf{u}_\ell^1 := [u_{2\ell+1}^1, u_{2\ell+2}^1], \quad \mathbf{u}_\ell^2 := [u_{2\ell+1}^2, u_{2\ell+2}^2], \quad \ell = 0, 1, \cdots, 6n.$$

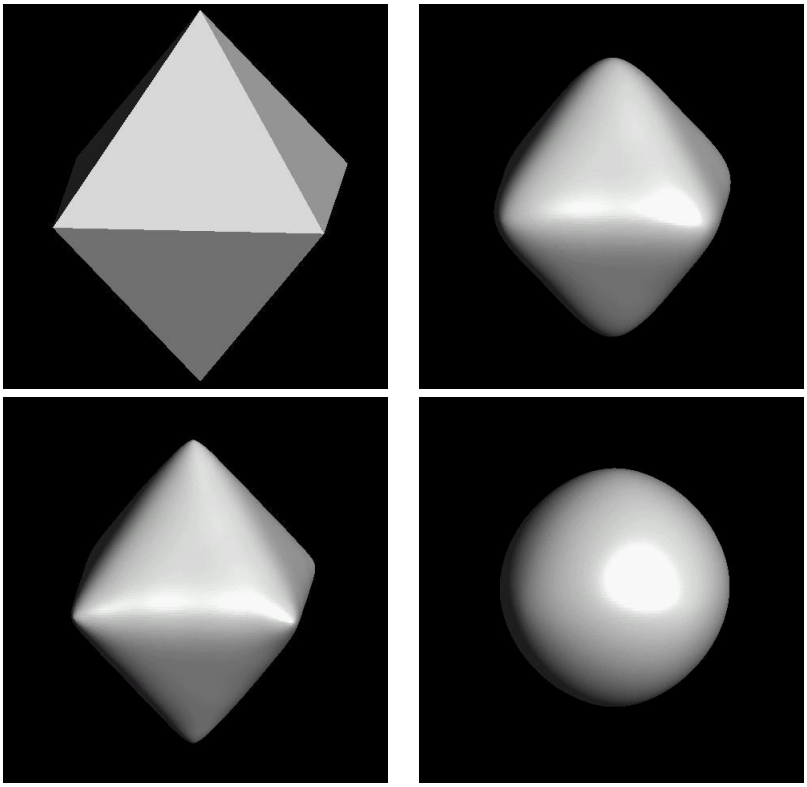

Figure 5: *Initial mesh (top-left), limiting surfaces by S_3^2-subdivision scheme with $x_4 = -\frac{1}{8}$ (top-right) and $x_4 = \frac{1}{16}$ (bottom-left), and limiting surface by Loop's scheme (bottom-right)*

Then the initial control vectors are given by

$$\mathbf{v}_i^0 := \begin{bmatrix} \mathbf{u}_i^1 \\ \mathbf{u}_i^2 \end{bmatrix} \in \mathbb{R}^{2\times 2}, \quad i = 0, 1, \cdots .$$

Let $\mathbf{v}_i^m$ be the vectors obtained after applying m iterations of the subdivision scheme (for the regular vertices) to $\mathbf{v}_i^0$. Then the first components v_i^m of $\mathbf{v}_i^m$ would converge to the characteristic map (see [20] for the scalar setting). In Fig.6, with $x_4 = \frac{1}{16}$, we show the meshes with vertices v_i^3 (namely, after 3 subdivision iterations), for extraordinary vertices with valences $n = 3, n = 5, n = 4, n = 7$. Observe that self-intersection does not occur. Therefore, these illustrations suggest the regularity and injectivity of the characteristic maps.

Observe that the (1, 1)-entries of $P_{0,0}, X, Y, Z, W, W_n$ are exactly the same as the weights of the templates for Loop's scheme. Therefore, S_3^2-subdivision could be considered as an extension of Loop's scheme. To confirm the validity of the extension, let $\mathbf{v}^m$ denote the set of vectors after m subdivision iteration steps. If S denotes the subdivision operator (in the sense that $\mathbf{v}^{m+1} = S\mathbf{v}^m$), then by considering the projection operator

$$Q : \{\mathbf{v_k} = [v_\mathbf{k},\ s_{1,\mathbf{k}}]\} \to \{[v_\mathbf{k},\ 0]\},$$

it is easy to see that $Q(SQ)^m\{\mathbf{v}_\mathbf{k}^0\}$ generates the same 3-D surface as Loop's scheme. By applying the S_3^2-subdivision, since $\mathbf{v}_\mathbf{k}^0 = [v_\mathbf{k}^0, s_{1,\mathbf{k}}^0]$, where $\{v_\mathbf{k}^0\}$ denotes the set of control

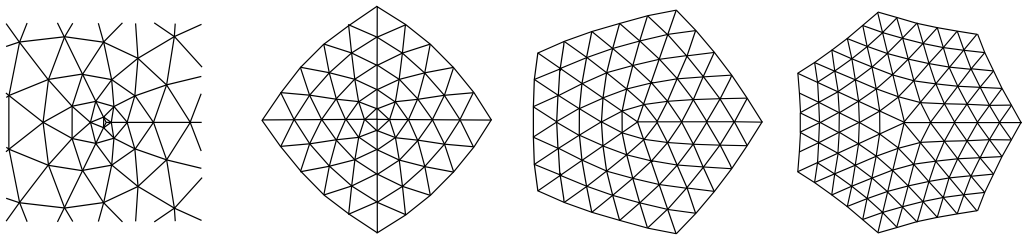

Figure 6: *Control meshes after 3 iterations for "Characteristic maps" of S_3^2-subdivision scheme with valence $n = 3, 4, 5, 7$*

points (or vertices of the control net), we gain a set of control parameters $\{s^0_{1,\mathbf{k}}\}$ for adaptive application of Loop's subdivision scheme. In this regard, we remark that it was illustrated in [5] that the geometry of the subdivision surfaces could change dramatically, by considering various choices of these parameters. For this reason, a guide to selecting initial choices of control parameters is provided in [5]. Finally, since S_3^2-subdivision engages piecewise polynomials of degree 3 as compared with polynomials of degree 4 of the box-spline B_{222} for Loop's scheme, it is perhaps less costly to evaluate exact values of the limiting S_3^2-subdivision surfaces than the subdivision surfaces obtained by applying Loop's scheme.

4. From Loop's scheme to interpolatory subdivisions

The extension of Loop's scheme to S_3^2-subdivision does not achieve the interpolatory feature. In Section 2, by applying the criterion of interpolatory subdivision matrices introduced in [4], we manipulate the S_3^2 refinement function vector to achieve surface interpolation for regular vertices. In this section, we will take care of extraordinary vertices with arbitrary valences, again with the interpolation property.

Let $\phi_0^b, \widetilde{\phi}_1^b$ be the splines defined in Section 2. Then as discussed in Section 2, $[\phi_0^b,\ \widetilde{\phi}_1^b]^T$ is also refinable with respect to the dilation matrices $2I_2$ and its refinement mask gives rise to an interpolatory scheme. The constant vector $\mathbf{y}_0$ for $[\phi_0^b,\ \widetilde{\phi}_1^b]^T$ to preserve all non-zero constants is $[1, \frac{1}{2}]$. In the following, in order to change $\mathbf{y}_0$ to $[1, 0]$, we further normalize $[\phi_0^b,\ \widetilde{\phi}_1^b]^T$ to $\Phi^c := [\phi_0^b + \frac{1}{2}\widetilde{\phi}_1^b,\ \widetilde{\phi}_1^b]^T$, which is again $2I_2$-refinable with some corresponding interpolatory refinement mask. The interpolatory templates generated by this mask are shown in Fig. 7, where

$$G_{0,0} = \begin{bmatrix} 1 & \frac{3}{8} \\ 0 & -\frac{1}{2} \end{bmatrix},\ J = \begin{bmatrix} \frac{31}{72} & -\frac{1}{36} \\ \frac{13}{36} & \frac{7}{36} \end{bmatrix},\ K = \begin{bmatrix} \frac{7}{72} & \frac{1}{72} \\ \frac{7}{36} & \frac{1}{36} \end{bmatrix},$$
$$L = \begin{bmatrix} 0 & -\frac{1}{16} \\ 0 & -\frac{1}{8} \end{bmatrix},\ M = \begin{bmatrix} -\frac{1}{144} & \frac{1}{288} \\ -\frac{1}{72} & \frac{1}{144} \end{bmatrix},\ N = \begin{bmatrix} -\frac{1}{72} & \frac{1}{144} \\ -\frac{1}{36} & \frac{1}{72} \end{bmatrix}.$$

This interpolatory subdivision scheme is still spline-based (since each component of Φ^c is a C^2 cubic spline), and will be called "S_3^2-interpolatory-subdivision" in our discussions.

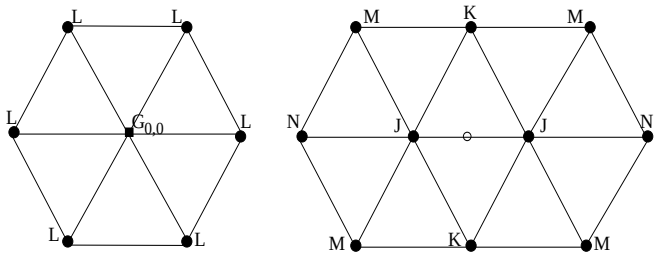

Figure 7: *Templates of C^2 cubic spline-based interpolatory scheme for regular vertices (left) and edge vertices (right)*

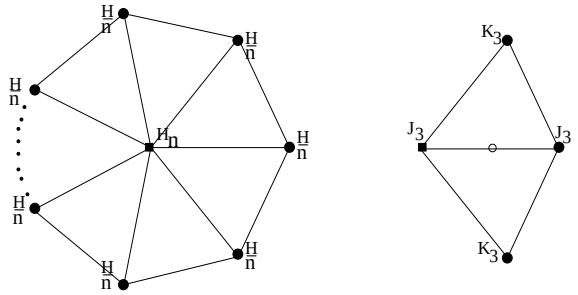

Figure 8: *Templates of C^2 spline interpolatory scheme for extraordinary vertices of valence n (left) and for edge vertices adjacent to an extraordinary vertex (right)*

For extraordinary vertices with arbitrary valences n, we will construct the matrix-valued weights for the templates shown in Fig.8, where

$$J_3 = \begin{bmatrix} \frac{31}{72}s & 0 \\ \frac{1}{4} & \frac{7}{36} \end{bmatrix},\ K_3 = \begin{bmatrix} \frac{1}{2} - \frac{31}{72}s & 0 \\ \frac{1}{4} & \frac{1}{36} \end{bmatrix},$$

for some $0 < s \leq \frac{36}{31}$, and

$$H_n = \begin{bmatrix} 1 & \frac{\alpha}{16} \\ 0 & x_2 \end{bmatrix},\ H = \begin{bmatrix} 0 & -\frac{\alpha}{16} \\ 0 & -\frac{27}{8(54-31s)}\alpha \end{bmatrix},$$

for some $\alpha, x_2 \in \mathbb{R}$. To determine s, x_2, and α, we analyze the spectral property of the subdivision matrix, to be denoted by S_G, on a 3-ring neighborhood of an extraordinary vertex of valence n. With careful labeling as in [19], certain appropriate permutations are applied to the DFT of S_G. Then from the derivation given in the appendix, we may conclude that S_G is similar to a block diagonal matrix with diagonal blocks, N_j,

$0 \le j \le n-1$, given by

$$N_0 = \begin{bmatrix} H_n & J_3 & L & K & N & M & M \\ H & J_3+2K_3 & G_{0,0}+2L & 2J+2M & J+2M & J+N+K & K+N+J \\ \mathbf{0} & \mathbf{0} & L & 2M & J & K+M & M+K \\ \mathbf{0} & \mathbf{0} & 2L & K+2N & 2K & J+M & J+M \\ \mathbf{0} & \mathbf{0} & \mathbf{0} & \mathbf{0} & N & \mathbf{0} & \mathbf{0} \\ \mathbf{0} & \mathbf{0} & \mathbf{0} & \mathbf{0} & M & M & N \\ \mathbf{0} & \mathbf{0} & \mathbf{0} & \mathbf{0} & M & N & M \end{bmatrix}, \tag{4.1}$$

and

$$N_j = \begin{bmatrix} J_3+K_3(z^j+\frac{1}{z^j}) & G_{0,0}+L(z^j+\frac{1}{z^j}) & J(1+z^j)+M(\frac{1}{z^j}+z^{2j}) & J+M(\frac{1}{z^j}+z^j) & J+\frac{N}{z^j}+Kz^j & K+Nz^{2j}+Jz^j \\ \mathbf{0} & L & M(1+z^j) & J & K+Mz^j & M+Kz^j \\ \mathbf{0} & L(1+\frac{1}{z^j}) & K+N(z^j+\frac{1}{z^j}) & K(1+\frac{1}{z^j}) & J+\frac{M}{z^j} & J+Mz^j \\ \mathbf{0} & \mathbf{0} & \mathbf{0} & N & \mathbf{0} & \mathbf{0} \\ \mathbf{0} & \mathbf{0} & \mathbf{0} & M & M & N \\ \mathbf{0} & \mathbf{0} & \mathbf{0} & \frac{M}{z^j} & N & M \end{bmatrix}, \tag{4.2}$$

where $1 \le j \le n-1$.

Here, by direction calculations, it can be shown that the constant matrices K, L, M, N satisfy the property that, for each $0 \le j \le n-1$,

$$\begin{bmatrix} N & \mathbf{0} & \mathbf{0} \\ M & M & N \\ \frac{M}{z^j} & N & M \end{bmatrix}$$

has only zero eigenvalues, and

$$\begin{bmatrix} L & M(1+z^j) \\ L(1+\frac{1}{z^j}) & K+N(z^j+\frac{1}{z^j}) \end{bmatrix}$$

has only two non-zero eigenvalues: $\frac{1}{8}$ and $-\frac{1}{8}$. Since for $1 \le j \le n-1$, $J_3+K_3(z^j+\frac{1}{z^j})$ has eigenvalues $\frac{31}{72}s+(1-\frac{31}{36}s)\cos\frac{2\pi j}{n}$ and $\frac{7}{36}+\frac{1}{18}\cos\frac{2\pi j}{n}$, it follows that the non-zero eigenvalues of S_G are precisely those of the matrix $\begin{bmatrix} H_n & J_3 \\ H & J_3+2K_3 \end{bmatrix}$ as well as the values

$$\frac{1}{8} \text{ (with multiplicity } n), \quad -\frac{1}{8} \text{ (with multiplicity } n),$$
$$\frac{31}{72}s+(1-\frac{31}{36}s)\cos\frac{2\pi j}{n}, \quad \frac{7}{36}+\frac{1}{18}\cos\frac{2\pi j}{n}, \quad 1 \le j \le n-1.$$

Here, the eigenvalues of

$$\begin{bmatrix} H_n & J_3 \\ H & J_3+2K_3 \end{bmatrix}$$

are $1, \frac{1}{4}$ and two more eigenvalues denoted as λ_+, λ_-. Hence, analogous to Loop's scheme and the S_3^2-subdivision scheme, we may choose

$$\lambda_+ = (\frac{31}{72}s+(1-\frac{31}{36}s)\cos\frac{2\pi}{n})^2.$$

λ_-	x_2	α
0	$\frac{31}{72}s-1+k^2$	$\frac{4}{81}\frac{29791s^3-190278s^2+69192s^2k^2+401760s-281232k^2s+279936(k^2-1)}{124s-405}$
$\frac{1}{32}$	$\frac{31}{72}s-\frac{31}{32}+k^2$	$\frac{31}{81}\frac{3844s^3-24273s^2+8928s^2k^2+50706s-35640sk^2+34992(k^2-1)}{124s-405}$
$\frac{1}{16}$	$\frac{31}{72}s-\frac{15}{16}+k^2$	$\frac{2}{81}\frac{59582s^3-371907s^2+138384s^2k^2+768366s-542376sk^2+524880(k^2-1)}{124s-405}$
$\frac{1}{8}$	$\frac{31}{72}s-\frac{7}{8}+k^2$	$\frac{4}{81}\frac{29791s^3-181629s^2+69192s^2k^2+366606s-261144sk^2+244944*(k^2-1)}{124s-405}$

Table 1: Possible choices of x_2, α, with $k^2 := (\frac{31}{72}s + (1-\frac{31}{36}s)\cos\frac{2\pi}{n})^2$

As to λ_-, we may allow it to be sufficiently small to facilitate the selection of x_2 and α. In Table 1, we list four possible choices of λ_- and the corresponding values of x_2, α.

In this table, we note that s is a free parameter with $0 < s \leq \frac{36}{31}$. We may just choose $s = \frac{36}{31}$. For example with this s and setting $\lambda_- = 0$, we have

$$x_2 = -\frac{1}{4},\ \alpha = \frac{64}{29}.$$

We may also choose other s smaller than $\frac{36}{31}$. For example, if we set $s = \frac{34}{31}$ and $\lambda_- = 0$, then

$$x_2 = (\frac{17}{36} + \frac{1}{18}\cos\frac{2\pi}{n})^2 - \frac{19}{36}, \quad \alpha = \frac{115520}{21789} - \frac{24320}{2421}(\frac{17}{36} + \frac{1}{18}\cos\frac{2\pi}{n})^2. \tag{4.3}$$

For these choices of x_2, α, the eigenvalues of S_G satisfy the property

$$\lambda_0 = 1, \quad \lambda_1 = \lambda_2, \quad |\lambda_3| < |\lambda_1|,$$

from which we can conclude that the subdivision surfaces are at least C^1, provided that their characteristic maps are regular and injective [15, 5]. In Fig. 9, for the scheme with x_2, α given in (4.3), we show the 2-dimensional meshes of v_i^3 near the extraordinary vertices with valences $n = 3, n = 4, n = 5, n = 7$, after this subdivision scheme is applied to the control vectors $\mathbf{v}_i^0$ constructed from the eigenvectors of the subdominant eigenvalues of the subdivision matrix S_G as described in Section 3. Observe that these meshes suggest the desired regularity and injectivity properties of the characteristic maps.

5. 1-ring C^2 interpolatory schemes

The edge template of the S_3^2-interpolatory-subdivision, based on bivariate C^2 cubic splines, introduced in Section 4 is no longer 1-ring. On the other hand, non-spline 1-ring C^2 interpolatory surface subdivision schemes have been introduced in our recent work [4]. The subdivision templates for regular vertices from one of these schemes are shown

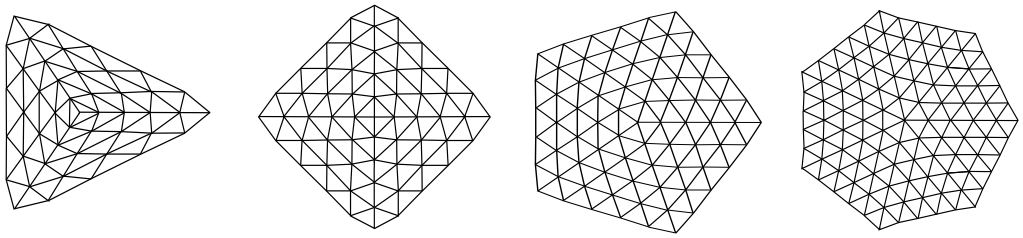

Figure 9: *Control meshes after 3 iterations for "Characteristic maps" of cubic spline-based interpolatory scheme with valence* $n = 3, n = 4, n = 5, n = 7$

in the first and second of the three templates in Fig.10, where the matrix-valued weights are given by

$$P_0 = \begin{bmatrix} 1 & -\frac{435}{256} \\ 0 & -\frac{91}{256} \end{bmatrix},\ D = \begin{bmatrix} 0 & \frac{145}{512} \\ 0 & -\frac{45}{512} \end{bmatrix},\ B = \begin{bmatrix} \frac{3}{8} & 0 \\ -\frac{47}{512} & \frac{69}{512} \end{bmatrix},\ C = \begin{bmatrix} \frac{1}{8} & 0 \\ -\frac{17}{512} & -\frac{5}{512} \end{bmatrix}. \tag{5.1}$$

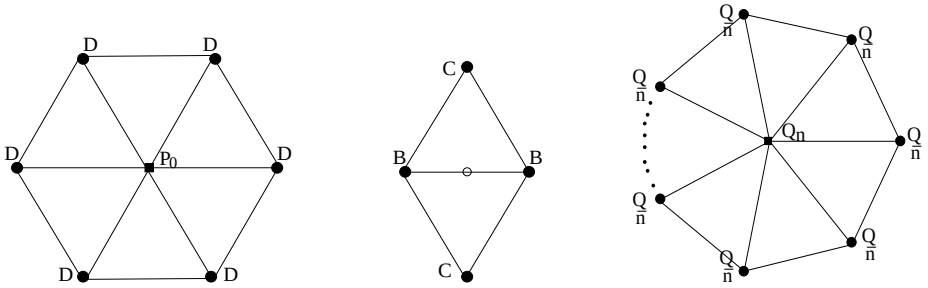

Figure 10: *Templates of 1-ring* C^2 *interpolatory scheme for regular vertices, edge vertices, extraordinary vertices of valence* n

The objective of this section is to derive the corresponding templates for extraordinary vertices for this particular 1-ring interpolatory scheme, which we will call "1-ring-interpolatory-subdivision" for later discussions. The templates to be constructed are shown on the right among the three templates in Fig.10. Here, we write

$$Q = \beta D = \begin{bmatrix} 0 & \frac{145}{512}\beta \\ 0 & -\frac{45}{512}\beta \end{bmatrix}, \quad Q_n = \begin{bmatrix} 1 & -\frac{145}{512}\beta \\ 0 & x_1 \end{bmatrix}. \tag{5.2}$$

Analogous to the previous discussions, to determine β, x_1, we consider the subdivision matrix $\widetilde{S}_P$ of this interpolatory scheme on a 3-ring neighborhood of the extraordinary vertex with valence n. Since this scheme has exactly the same template sizes as those of the S_3^2-subdivision scheme, the formulation of $\widetilde{S}_P$ follows immediately from the subdivision matrix S_P for S_3^2-subdivision scheme, with $P_{0,0}, X, Y, Z, W_n, W$ replaced by P_0, B, C, D, Q_n, Q, respectively. Hence, from the discussion on S_P in Section 3, we know

that $\widetilde{S}_P$ is similar to a block diagonal matrix with the diagonal blocks, O_j, $0 \le j \le n-1$, given by

$$O_0 = \begin{bmatrix} o_0 & * \\ 0_{6\times 8} & 0_6 \end{bmatrix}, \qquad O_j = \begin{bmatrix} o_1(z^j) & * \\ 0_6 & 0_6 \end{bmatrix}, \quad 1 \le j \le n-1, \tag{5.3}$$

where

$$o_0 = \begin{bmatrix} Q_n & B & D & C \\ Q & B+2C & P_0+2C & 2B \\ \mathbf{0} & \mathbf{0} & D & \mathbf{0} \\ \mathbf{0} & \mathbf{0} & 2D & C \end{bmatrix},$$

$$o_1(z) = \begin{bmatrix} B + C(z+\frac{1}{z}) & P_0 + D(z+\frac{1}{z}) & B(1+z) \\ \mathbf{0} & D & \mathbf{0} \\ \mathbf{0} & D(1+\frac{1}{z}) & C \end{bmatrix}.$$

Observe that D has only one non-zero eigenvalue $-\frac{45}{512}$ and C has two non-zero eigenvalues $\frac{1}{8}$ and $-\frac{5}{512}$, and that

$$B + C(z^j + \frac{1}{z^j}) = \begin{bmatrix} \frac{3}{8} + \frac{1}{4}\cos\frac{2\pi j}{n} & 0 \\ -\frac{47}{512} - \frac{17}{256}\cos\frac{2\pi j}{n} & \frac{69}{512} - \frac{5}{256}\cos\frac{2\pi j}{n} \end{bmatrix}.$$

Thus, the non-zero eigenvalues of $\widetilde{S}_P$ are consist of the eigenvalues of the matrix $\begin{bmatrix} Q_n & B \\ Q & B+2C \end{bmatrix}$ as well as the values

$$-\frac{45}{512} \text{ (with multiplicty } n-1), \quad \frac{1}{8} \text{ (with multiplicty } n-1), \quad -\frac{5}{512} \text{ (with multiplicty } n-1),$$

$$\frac{3}{8} + \frac{1}{4}\cos\frac{2\pi j}{n}, \quad \frac{69}{512} - \frac{5}{256}\cos\frac{2\pi j}{n}, \quad 1 \le j \le n-1.$$

For the Q and Q_n in (5.2), the eigenvalues of $\begin{bmatrix} Q_n & B \\ Q & B+2C \end{bmatrix}$ are given by $1, \frac{59}{512}$, and

$$\lambda_\pm = \frac{5}{16} + \frac{x_1}{2} \pm \frac{1}{64}\sqrt{400 - 1280x_1 + 1024x_1^2 - 155\beta}.$$

Analogous to Loop's scheme and S_3^2-subdivision, we may set

$$\lambda_+ = (\frac{3}{8} + \frac{1}{4}\cos\frac{2\pi}{n})^2,$$

and choose a sufficiently small value of λ_- to facilitate the selection of x_1 and β.

For example, if we set $\lambda_- = 0$, then we have

$$x_1 = -a, \quad \beta = \frac{512}{31}a,$$

where the value of a, as given in (1.3), is a function of the valence n.

If we choose $\lambda_- = \frac{5}{256}$, then we have

$$x_1 = -\frac{155}{256} + (\frac{3}{8} + \frac{1}{4}\cos\frac{2\pi}{n})^2, \quad \beta = 10 - 16(\frac{3}{8} + \frac{1}{4}\cos\frac{2\pi}{n})^2.$$

For this particular choice of $\lambda_-(= \frac{5}{256})$, it is worthwhile to mention that by setting $n = 6$, Q_n and Q are exactly the same as the weights P_0 and $6D$ for regular vertices, as given in (5.1), respectively.

In the following, let us consider the simpler case $\lambda_- = 0$, and choose

$$Q = \frac{512}{31}aD, \quad Q_n = \begin{bmatrix} 1 & -\frac{145}{31}a \\ 0 & -a \end{bmatrix}, \tag{5.4}$$

where D is again the matrix given in (5.1) and the formula of a is given in (1.3). For this particular choice, the eigenvalues of the corresponding subdivision matrix satisfy $\lambda_0 = 1, \lambda_1 = \lambda_2$ with $|\lambda_1| < 1$ and $|\lambda_j| < |\lambda_1|$, $j = 3, 4, \cdots$. Therefore, if the corresponding characteristic map is regular and injective, then the scheme is at least C^1 for extraordinary vertices of arbitrary valence n. In Fig.11, we show the 2-dimensional meshes of v_i^3 near the extraordinary vertices with valences $n = 3, n = 4, n = 5, n = 7$, after this 1-ring interpolatory subdivision scheme is applied to the (initial) control vectors $\mathbf{v}_i^0$ that are constructed from the eigenvectors of the subdominant eigenvalues of the subdivision matrix $\widetilde{S}_P$ as described in Section 3. Again, these meshes suggest the regularity and injectivity properties of the characteristic maps.

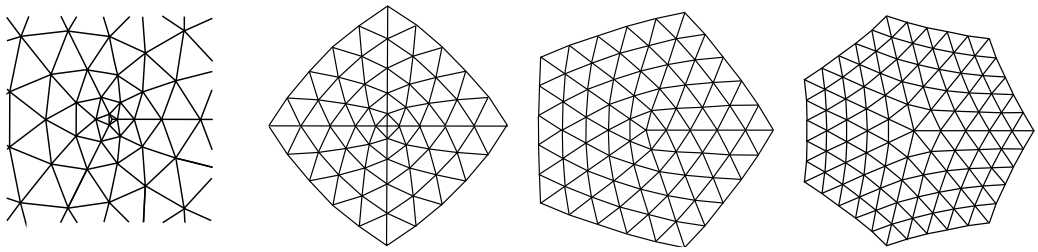

Figure 11: *Control meshes after 3 iterations for "Characteristic maps" of 1-ring interpolatory scheme with valences* $n = 3, n = 4, n = 5, n = 7$

Since the constant vector y_0 for reproduction of constants is given by $[1, 0]$, it is tempting to set $s^0_{\mathbf{k},1} = \mathbf{0}$. For example, for the initial triangular control net of saddle shape as shown on the top-left picture of Fig. 12, we obtain the subdivision surface shown in the top-middle figure by applying the interpolatory scheme in Fig. 10 to control vectors with control vertices of this net as the first columns, and $\mathbf{0}$ as the second columns. This requires 5 iterative steps, with a zoom-in picture shown on the top-right figure to illustrate the detail of the surface. For comparison, the modified butterfly scheme [22] is applied, again using 5 iterative steps, to yield the subdivision surface and its zoom-in picture to the same region, shown on the bottom-left and bottom-right figures, respectively.

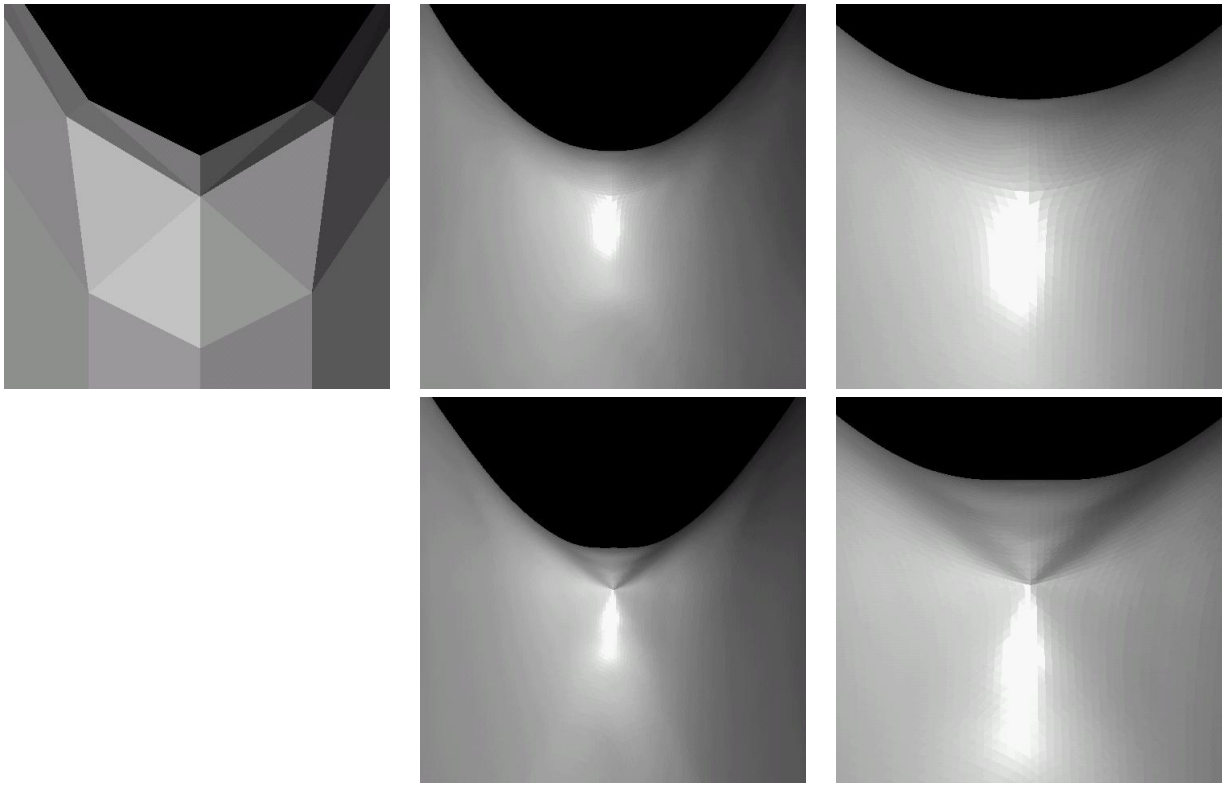

Figure 12: *Control net (top-left), and subdivided surface (top-middle) and zoom-in part (top-right) by 1-ring interpolatory scheme in Fig. 10, and subdivided surface (bottom-left) and zoom-in part (bottom-right) by modified butterfly scheme*

However, it does not seem to be a good idea to set the shape control parameters to be $\mathbf{0}$ in general, particularly when the 1-ring interpolatory scheme is applied to control vertices that are "corner" vertices of a polyhedron. The reason is that since new vertices generated from each iterative step always lie on the subdivision surface, the first few iterative steps are particularly important in determining the geometric shape of the subdivision surface. In Appendix II, we will explain why shape control parameters

$$s_{j,1}^0 = -t_j v_j^0$$

with t_j in $(0, 2]$ could be preferable choices for this type of control vertices v_j^0 . In general, however, since surface geometry is very sensitive to the change of shape control parameters, the choice of these parameters is an important issue. This problem will be addressed in our future work.

As an example, let us again consider the octahedron with vertices $v_j^0, 0 \leq j \leq 5$ shown on the top-left of Fig. 13 to be put in the first columns of the control vectors. Then applying the interpolatory scheme in Fig. 10 to the control vectors $(v_j^0, -2v_j^0), 0 \leq j \leq 5$, namely, by setting $t_j = 2$, we obtain the finer and finer meshes as shown in Fig. 13, after 1, 2, 3 iterations, respectively. The limiting surface is shown in the bottom-middle of Fig. 13. With the same octahedron on the top-left of Fig. 13 as the initial control

net, the modified butterfly scheme [22] is applied to render the limiting surface shown in the bottom-right picture of Fig. 13 for comparison.

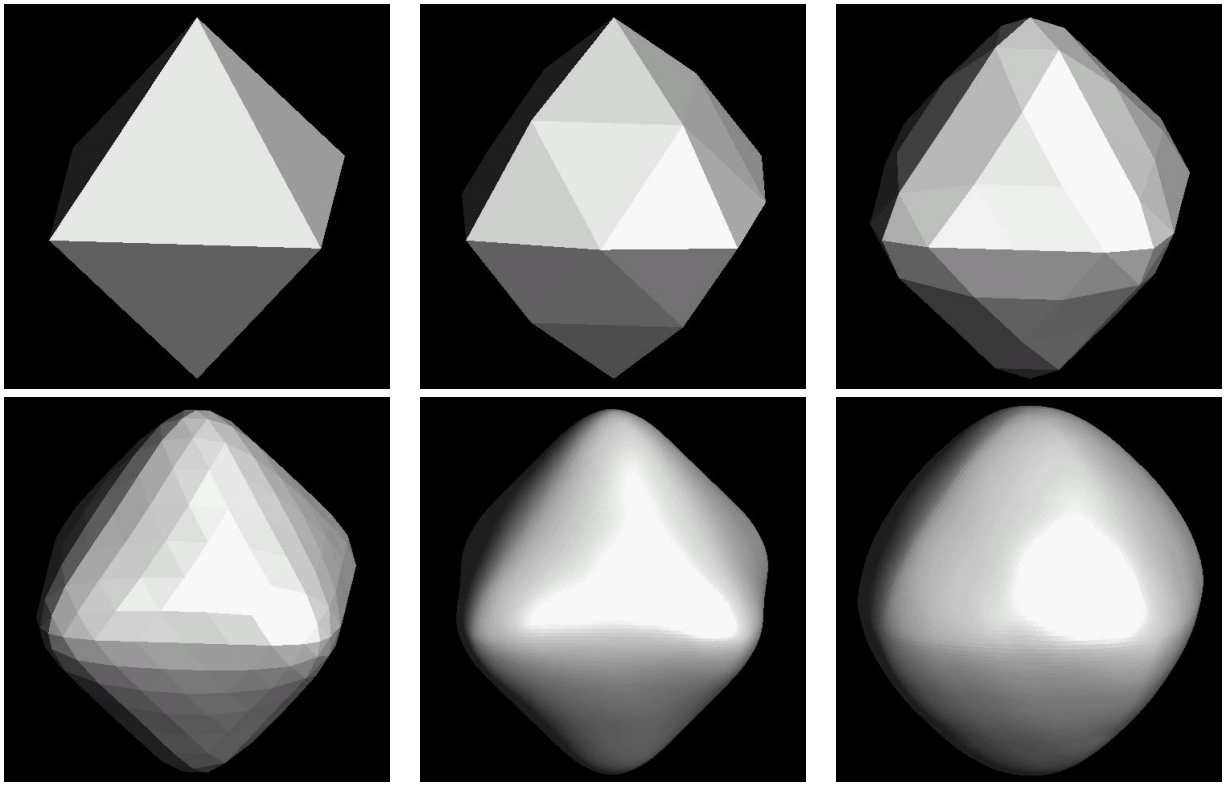

Figure 13: *Control net (octahedron, on top-left), finer meshes with 1, 2, 3 iteration steps, and limiting surface (bottom-middle) by 1-ring interpolatory scheme in Fig. 10, and limiting surface by modified butterfly scheme (bottom-right)*

6. Appendices

6.1. Appendix I: Spectral analysis

This subsection is devoted to the discussion of the spectral property of the subdivision matrices. The primary tool is the discrete Fourier transform (**DFT**). Although DFT of cyclic (block) matrices has been well studied in the literature, we include a brief discussion here for the convenience of the interested reader not familiar with the topic (see also [16]).

Let $\mathcal{C}$

$$\mathcal{C} = \begin{bmatrix} C_0 & C_1 & \cdots & C_{n-1} \\ C_{n-1} & C_0 & \cdots & C_{n-2} \\ \cdots & \cdots & \cdots & \cdots \\ C_1 & C_2 & \cdots & C_0 \end{bmatrix} \tag{6.1}$$

be a cyclic block matrix with $r \times r$ sub-matrix C_j blocks. Let $z = e^{\frac{2\pi}{n}i}$ and consider the

Kroncker product

$$U_n := \left[z^{kj}\right] \otimes I_r = \left[z^{kj} I_r\right]_{k=0,\cdots,n-1, j=0,\cdots,n-1};$$

of $\left[z^{kj}\right]$ with the identity matrix I_r. Then by direct calculations, the DFT of $\mathcal{C}$, defined by $\widehat{\mathcal{C}} := U_n \mathcal{C} U_n^{-1}$, can be written as

$$\widehat{\mathcal{C}} = \mathrm{diag}(\widehat{C}_0, \widehat{C}_1, \cdots, \widehat{C}_{n-1}),$$

with

$$\widehat{C}_j := \sum_{k=0}^{n-1} C_k z^{-jk}.$$

Observe that since the matrix $\mathcal{C}$ and its DFT $\widehat{\mathcal{C}}$ are similar to each other, they have the same eigenvalues.

In the following, we apply the DFT to transform the subdivision matrices of the S_3^2-subdivision and S_3^2-interpolatory-subdivision schemes into block diagonal matrices. The following notations are needed for our discussion. First, $\mathrm{diag}(M_0)$ will denote the matrix $\mathcal{C}$ defined in (6.1) with $C_j = 0, 1 \le j \le n-1$; that is, $\mathrm{diag}(C_0)$ is the diagonal block matrix with each diagonal block being C_0. Clearly, the DFT of $\mathrm{diag}(C_0)$ is itself. Next, $\mathcal{C}(C_0, C_1; C_{n-1})$ will denote the matrix $\mathcal{C}$ defined in (6.1), but with $C_j = 0, j \neq 0, 1, n-1$. Then, the DFT $\widehat{\mathcal{C}}(C_0, C_1; C_{n-1})$ of $\mathcal{C}(C_0, C_1; C_{n-1})$ is given by

$$\mathrm{diag}(C_0 + C_1 + C_{n-1}, C_0 + C_1 \frac{1}{z} + C_{n-1} z, \cdots, C_0 + C_1 \frac{1}{z^{n-1}} + C_{n-1} z^{n-1}).$$

We also use $\mathcal{C}(C_0, C_1; C_{n-2}, C_{n-1})$ to denote the matrix $\mathcal{C}$ defined in (6.1) with $C_j = 0, j \neq 0, 1, n-2, n-1$.

(i) Subdivision matrix of S_3^2-subdivision

With the order of labeling the indices as illustrated in Fig. 4, the subdivision matrix S_P of S_3^2-subdivision (with templates given in Fig. 3) on a 3-ring neighborhood of an extraordinary vertex with valence n, is

$$\begin{bmatrix}
W_n & [X, X, \cdots, X] & [Z, Z, \cdots, Z] & [Y, Y, \cdots, Y] & \mathbf{0} & \mathbf{0} & \mathbf{0} \\
\frac{1}{n}\begin{bmatrix} W \\ W \\ \vdots \\ W \end{bmatrix} & \mathcal{C}(X, Y; Y) & \mathcal{C}(P_{0,0}, Z; Z) & \mathcal{C}(X, \mathbf{0}; X) & \mathrm{diag}(X) & \mathcal{C}(X, \mathbf{0}; Y) & \mathcal{C}(Y, \mathbf{0}; X) \\
\mathbf{0} & \mathbf{0} & \mathrm{diag}(Z) & \mathbf{0} & \mathrm{diag}(X) & \mathrm{diag}(Y) & \mathcal{C}(\mathbf{0}, \mathbf{0}; Y) \\
\mathbf{0} & \mathbf{0} & \mathcal{C}(Z, Z; \mathbf{0}) & \mathrm{diag}(Y) & \mathcal{C}(Y, Y; \mathbf{0}) & \mathrm{diag}(X) & \mathrm{diag}(X) \\
\mathbf{0} & \mathbf{0} & \mathbf{0} & \mathbf{0} & \mathbf{0} & \mathbf{0} & \mathbf{0} \\
\mathbf{0} & \mathbf{0} & \mathbf{0} & \mathbf{0} & \mathbf{0} & \mathbf{0} & \mathbf{0} \\
\mathbf{0} & \mathbf{0} & \mathbf{0} & \mathbf{0} & \mathbf{0} & \mathbf{0} & \mathbf{0}
\end{bmatrix}.$$

Then $\mathcal{U} S_P \mathcal{U}^{-1}$, where

$$\mathcal{U} := \mathrm{diag}(I_2, U_n, U_n, \cdots, U_n)$$

is a 7×7 diagonal block matrix, is given by

$$\begin{bmatrix} W_n & [X,\mathbf{0},\cdots,\mathbf{0}] & [Z,\mathbf{0},\cdots,\mathbf{0}] & [Y,\mathbf{0},\cdots,\mathbf{0}] & \mathbf{0} & \mathbf{0} & \mathbf{0} \\ \begin{bmatrix} W \\ \mathbf{0} \\ \vdots \\ \mathbf{0} \end{bmatrix} & \widehat{\mathcal{C}}(X,Y;Y) & \widehat{\mathcal{C}}(P_{0,0},Z;Z) & \widehat{\mathcal{C}}(X,\mathbf{0};X) & \mathrm{diag}(X) & \widehat{\mathcal{C}}(X,\mathbf{0};Y) & \widehat{\mathcal{C}}(Y,\mathbf{0};X) \\ \mathbf{0} & \mathbf{0} & \mathrm{diag}(Z) & \mathbf{0} & \mathrm{diag}(X) & \mathrm{diag}(Y) & \widehat{\mathcal{C}}(\mathbf{0},\mathbf{0};Y) \\ \mathbf{0} & \mathbf{0} & \widehat{\mathcal{C}}(Z,Z;\mathbf{0}) & \mathrm{diag}(Y) & \widehat{\mathcal{C}}(Y,Y;\mathbf{0}) & \mathrm{diag}(X) & \mathrm{diag}(X) \\ \mathbf{0} & \mathbf{0} & \mathbf{0} & \mathbf{0} & \mathbf{0} & \mathbf{0} & \mathbf{0} \\ \mathbf{0} & \mathbf{0} & \mathbf{0} & \mathbf{0} & \mathbf{0} & \mathbf{0} & \mathbf{0} \\ \mathbf{0} & \mathbf{0} & \mathbf{0} & \mathbf{0} & \mathbf{0} & \mathbf{0} & \mathbf{0} \end{bmatrix}.$$

Next, let $\mathcal{L}$ denote the square matrix (operator) for exchanging $kn+j$ and $(j-2)6+k+2$ (block matrix) rows, where $0 \leq k \leq 5, 2 \leq j \leq n+1$. Then following [20] in exchanging (block matrix) rows, as well as the corresponding (block matrix) columns, of $\mathcal{U}S_P\mathcal{U}^{-1}$, we arrive at $\mathcal{L}\mathcal{U}S_P\mathcal{U}^{-1}\mathcal{L}^{-1}$, which is a block diagonal matrix with diagonal blocks given by

$$\begin{bmatrix} W_n & X & Z & Y & \mathbf{0} & \mathbf{0} & \mathbf{0} \\ W & X+2Y & P_{0,0}+2Z & 2X & X & X+Y & Y+X \\ \mathbf{0} & \mathbf{0} & Z & \mathbf{0} & X & Y & Y \\ \mathbf{0} & \mathbf{0} & 2Z & Y & 2Y & X & X \\ \mathbf{0} & \mathbf{0} & \mathbf{0} & \mathbf{0} & \mathbf{0} & \mathbf{0} & \mathbf{0} \\ \mathbf{0} & \mathbf{0} & \mathbf{0} & \mathbf{0} & \mathbf{0} & \mathbf{0} & \mathbf{0} \\ \mathbf{0} & \mathbf{0} & \mathbf{0} & \mathbf{0} & \mathbf{0} & \mathbf{0} & \mathbf{0} \end{bmatrix},$$

and

$$\begin{bmatrix} X+Y(z^j+\frac{1}{z^j}) & P_{0,0}+Z(z^j+\frac{1}{z^j}) & X(1+z^j) & X & X+Yz^j & Y+Xz^j \\ \mathbf{0} & Z & \mathbf{0} & X & Y & Yz^j \\ \mathbf{0} & Z(1+\frac{1}{z^j}) & Y & Y(1+\frac{1}{z^j}) & X & X \\ \mathbf{0} & \mathbf{0} & \mathbf{0} & \mathbf{0} & \mathbf{0} & \mathbf{0} \\ \mathbf{0} & \mathbf{0} & \mathbf{0} & \mathbf{0} & \mathbf{0} & \mathbf{0} \\ \mathbf{0} & \mathbf{0} & \mathbf{0} & \mathbf{0} & \mathbf{0} & \mathbf{0} \end{bmatrix},$$

where $1 \leq j \leq n-1$. Therefore, the subdivision matrix S_P is similar to a block diagonal matrix with diagonal blocks given by (3.4), as desired.

(ii) Subdivision matrix of S_3^2-interpolatory-subdivision

By using the same labeling as above, the subdivision matrix S_G of the S_3^2-interpolatory-subdivision, with templates given in Fig.7 and Fig.8, on a 3-ring neighborhood of an

extraordinary vertex with valence n, is

$$\begin{bmatrix} H_n & [J_3, J_3, \cdots, J_3] & [L, L, \cdots, L] & [K, K, \cdots, K] & [N, N, \cdots, N] & [M, M, \cdots, M] & [M, M, \cdots, M] \\ \frac{1}{n}\begin{bmatrix} H \\ H \\ \vdots \\ H \end{bmatrix} & \mathcal{C}(J_3, K_3; K_3) & \mathcal{C}(G_{0,0}, L; L) & \mathcal{C}(J, M; M, J) & \mathcal{C}(J, M; M) & \mathcal{C}(J, N; K) & \mathcal{C}(K, \mathbf{0}; N, J) \\ \mathbf{0} & \mathbf{0} & \mathrm{diag}(L) & \mathcal{C}(M, \mathbf{0}; M) & \mathrm{diag}(J) & \mathcal{C}(K, \mathbf{0}; M) & \mathcal{C}(M, \mathbf{0}; K) \\ \mathbf{0} & \mathbf{0} & \mathcal{C}(L, L; \mathbf{0}) & \mathcal{C}(K, N; N) & \mathcal{C}(K, K; \mathbf{0}) & \mathcal{C}(J, M; \mathbf{0}) & \mathcal{C}(J, \mathbf{0}; M) \\ \mathbf{0} & \mathbf{0} & \mathbf{0} & \mathbf{0} & \mathrm{diag}(N) & \mathbf{0} & \mathbf{0} \\ \mathbf{0} & \mathbf{0} & \mathbf{0} & \mathbf{0} & \mathrm{diag}(M) & \mathrm{diag}(M) & \mathrm{diag}(N) \\ \mathbf{0} & \mathbf{0} & \mathbf{0} & \mathbf{0} & \mathcal{C}(\mathbf{0}, M; \mathbf{0}) & \mathrm{diag}(N) & \mathrm{diag}(M) \end{bmatrix}$$

where for $n = 3$, the $(2, 4)$-block $\mathcal{C}(J, M; M, J)$ in the above block matrix is $\mathcal{C}(J, 2M; J)$. Withe the same 7×7 diagonal matrix $\mathcal{U}$ defined above, we see that $\mathcal{U}S_G\mathcal{U}^{-1}$ is given by

$$\begin{bmatrix} H_n & [J_3, \mathbf{0}, \cdots, \mathbf{0}] & [L, \mathbf{0}, \cdots, \mathbf{0}] & [K, \mathbf{0}, \cdots, \mathbf{0}] & [N, \mathbf{0}, \cdots, \mathbf{0}] & [M, \mathbf{0}, \cdots, \mathbf{0}] & [M, \mathbf{0}, \cdots, \mathbf{0}] \\ \begin{bmatrix} H \\ \mathbf{0} \\ \vdots \\ \mathbf{0} \end{bmatrix} & \widehat{\mathcal{C}}(J_3, K_3; K_3) & \widehat{\mathcal{C}}(G_{0,0}, L; L) & \widehat{\mathcal{C}}(J, M; M, J) & \widehat{\mathcal{C}}(J, M; M) & \widehat{\mathcal{C}}(J, N; K) & \widehat{\mathcal{C}}(K, \mathbf{0}; N, J) \\ \mathbf{0} & \mathbf{0} & \mathrm{diag}(L) & \widehat{\mathcal{C}}(M, \mathbf{0}; M) & \mathrm{diag}(J) & \widehat{\mathcal{C}}(K, \mathbf{0}; M) & \widehat{\mathcal{C}}(M, \mathbf{0}; K) \\ \mathbf{0} & \mathbf{0} & \widehat{\mathcal{C}}(L, L; \mathbf{0}) & \widehat{\mathcal{C}}(K, N; N) & \widehat{\mathcal{C}}(K, K; \mathbf{0}) & \widehat{\mathcal{C}}(J, M; \mathbf{0}) & \widehat{\mathcal{C}}(J, \mathbf{0}; M) \\ \mathbf{0} & \mathbf{0} & \mathbf{0} & \mathbf{0} & \mathrm{diag}(N) & \mathbf{0} & \mathbf{0} \\ \mathbf{0} & \mathbf{0} & \mathbf{0} & \mathbf{0} & \mathrm{diag}(M) & \mathrm{diag}(M) & \mathrm{diag}(N) \\ \mathbf{0} & \mathbf{0} & \mathbf{0} & \mathbf{0} & \mathcal{C}(\mathbf{0}, M; \mathbf{0}) & \mathrm{diag}(N) & \mathrm{diag}(M) \end{bmatrix}.$$

Again, we exchange both $kn + j$ and $(j - 2)6 + k + 2$ (block matrix) rows and (block matrix) columns of $\mathcal{U}S_G\mathcal{U}^{-1}$, $0 \le k \le 5, 2 \le j \le n + 1$, resulting in the matrix $\mathcal{L}\mathcal{U}S_G\mathcal{U}^{-1}\mathcal{L}^{-1}$, which is a block diagonal matrix with diagonal blocks given by (4.1) and (4.2). That is, the subdivision matrix S_G is similar to a block diagonal matrix with diagonal blocks given by (4.1) and (4.2), as desired.

6.2. Appendix II: Shape control parameters for 1-ring interpolatory subdivision

When the 1-ring-interpolatory-subdivision is applied to such vertices as those in the control net on the left of Fig. 14, the position of an edge vertex is determined by 4 control vectors, $\mathbf{v}_0^0, \mathbf{v}_1^0, \mathbf{v}_2^0, \mathbf{v}_3^0$, say, with first components $\mathsf{u}_0, \mathsf{u}_1, \mathsf{u}_2, \mathsf{u}_3$, respectively, which are among the vertices of the control net. Let $s_0^0, s_1^0, s_2^0, s_3^0$ denote the control parameters (i.e. second components of the control vectors) and u^1 a new vertex, after one iteration, that corresponds to the mid-point $\mathsf{v}_0 = \frac{1}{2}(\mathsf{u}_0 + \mathsf{u}_1)$ (indicated by a $\circ$ in both pictures in Fig. 14) of the edge $[\mathsf{u}_0, \mathsf{u}_1]$ of the control net. Notice that the (1, 1)-entries of B and C are $\frac{3}{8}$ and $\frac{1}{8}$, respectively. So, if all of the control parameters $s_0^0, s_1^0, s_2^0, s_3^0$ are set to be $[0, 0, 0]^T$, then the position u^1 (indicated by $\bullet$ on the right of Fig. 14) could be a little too far away from v_0, indicated by $\circ$ in the same picture. But since this scheme is interpolatory, u^1 also lies on the subdivision surface. Therefore, it is almost certain that

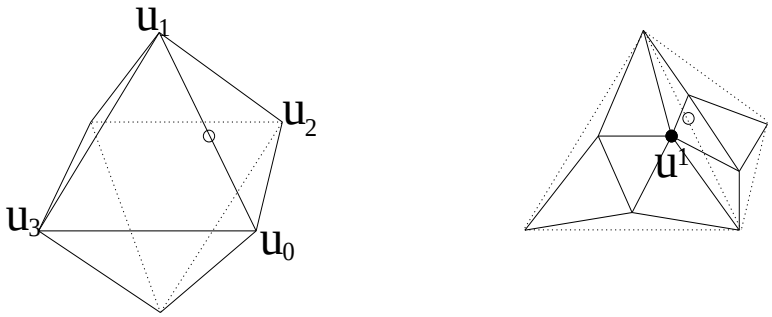

Figure 14: *Finer mesh (right picture), after one iteration applied to triangles* $\triangle \mathsf{u}_0\mathsf{u}_1\mathsf{u}_3$ *and* $\triangle \mathsf{u}_0\mathsf{u}_1\mathsf{u}_2$ *(left picture), with vertex* u^1 *(right picture) corresponding to the* $\circ$ *on the edge* $[\mathsf{u}_0, \mathsf{u}_1]$*(left picture)*

the limiting surface could be undesirably wavy. For this reason, it is not advisable to set all control parameters s_j^0 to be $[0, 0, 0]^T$, in general.

On the other hand, for any upper triangular matrix

$$U = \begin{bmatrix} 1 & -t \\ 0 & 1 \end{bmatrix}, \tag{6.1}$$

with $t \in \mathbb{R}$, where the matrix weights

$$\begin{aligned} &P_{\mathsf{v}} := UP_0U^{-1},\ D_{\mathsf{v}} := UDU^{-1},\ B_{\mathsf{v}} := UBU^{-1}, \\ &C_{\mathsf{v}} := UCU^{-1},\ Q_{\mathsf{n},\mathsf{v}} := UQ_{\mathsf{n}}U^{-1},\ Q_{\mathsf{v}} := UQU^{-1}, \end{aligned} \tag{6.2}$$

provide another interpolatory scheme with templates shown in Fig. 15. This scheme generates subdivision surfaces with the same order of smoothness as that of the surfaces generated by P_0, D, B, C, Q_n, Q.

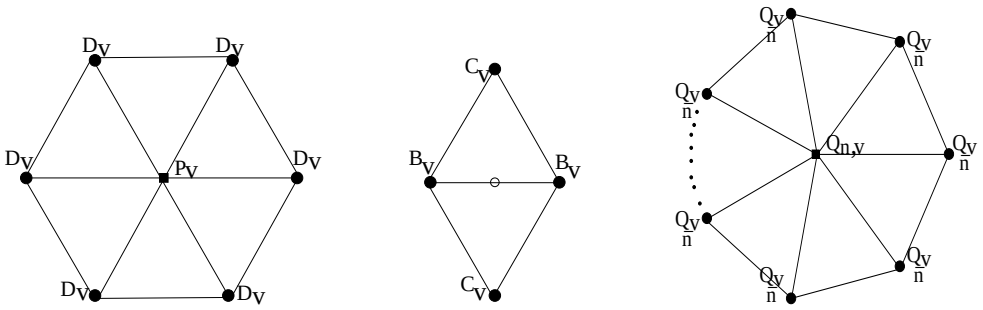

Figure 15: *Templates of 1-ring interpolatory matrix-valued scheme for regular vertices, edge vertices, and extraordinary vertices*

For the new weights $P_{\mathsf{v}}, D_{\mathsf{v}}, B_{\mathsf{v}}, C_{\mathsf{v}}, Q_{\mathsf{n},\mathsf{v}}, Q_{\mathsf{v}}$ in (6.2), obtained by a similar transformation with the matrix U that carries a free parameter t, observe that the (1, 1)-entries of $B_{\mathsf{v}}, C_{\mathsf{v}}$ are $\frac{3}{8} + \frac{47}{517}t$ and $\frac{1}{8} + \frac{17}{517}t$, respectively. Hence, for $\frac{3}{8} + \frac{47}{517}t$, if we choose the value of t so that $\frac{3}{8} + \frac{47}{517}t$ is close to $\frac{1}{2}$, then u^1 would be close to v_0. On the other hand,

for positive values of t, $\frac{1}{8} + \frac{17}{517}t$ is significantly larger than 0, which implies that u^1 is far away from v_0. Fortunately, since the value $\frac{47}{517}$ is greater than $\frac{17}{517}$ by a factor of 3, it is still advisable to choose a positive value of t. Indeed, a positive t should imply less oscillation in the limiting surface. For this reason, we conclude that appropriate values of t in the interval $(0, 2]$ should be good choices, in general.

For an initial mesh with control points $\{v_j^0\}_j$ (i.e. the control net with $\{v_j^0\}_j$ as vertices), it can be shown that the subdivision surface generated by the 1-ring-interpolatory-subdivision scheme, with weights P_0, D, B, C, Q_n, Q, applied to the control vectors $\{(v_j^0, -tv_j^0)\}_j$ is identical to the subdivision surface generated by the scheme, with weights $P_\mathsf{v}, D_\mathsf{v}, B_\mathsf{v}, C_\mathsf{v}, Q_{\mathsf{n},\mathsf{v}}, Q_\mathsf{v}$, applied to the control vectors $\{(v_j^0, \mathbf{0})\}_j$. In other words, for a suitable choice of t, one could apply the templates in Fig.10 with initial control vectors $\{(v_j^0, -tv_j^0)\}_j$, or equivalently, the templates in Fig.15 with initial control vectors $\{(v_j^0, \mathbf{0})\}_j$. Therefore, from this observation and the discussion in the previous paragraph, shape control parameters $s_{j,1}^0 = -t_j v_j^0$ with some suitable t_j in $(0, 2]$ should be good choices for control vertices v_j^0 of the same type as those illustrated on the left of Fig. 14.

References

[1] E. Catmull and J. Clark, Recursively generated B-splines surfaces on arbitrary topological meshes, *Comput. Aided Design* 10 (1978), 350–355.

[2] C.K. Chui and Q.T. Jiang, Surface subdivision schemes generated by refinable bivariate spline function vectors, *Appl. Comput. Harmonic Anal.* 15 (2003), 147–162.

[3] C.K. Chui and Q.T. Jiang, Refinable bivariate C^2-splines for multi-level data representation and surface display, *Math Comp.* 74 (2005), 1369–1390.

[4] C.K. Chui and Q.T. Jiang, Matrix-valued symmetric templates for interpolatory surface subdivisions I. Regular vertices, *Appl. Comput. Harmonic Anal.* 19 (2005), 303–339.

[5] C.K. Chui and Q.T. Jiang, Matrix-valued subdivision schemes for generating surfaces with extraordinary vertices, *Comput. Aided Geom. Design* 23 (2006), 419–438.

[6] C.K. Chui and Q.T. Jiang, Refinable bivariate quartic and quintic C^2-splines for quadrilateral subdivisions, *J. Comput. Appl. Math.* 196 (2006), 402–424.

[7] D.W.H. Doo and M.A. Sabin, Analysis of the behaviour of recursive division surfaces near extraordinary points, *Computer Aided Design* 10 (1978), 356–360.

[8] N. Dyn, J.A. Gregory, and D. Levin, A butterfly subdivision scheme for surface interpolation with tension control, *ACM Trans. Graphics* 2 (1990), 160–169.

[9] B. Han, T. Yu, and B. Piper, Multivariate refinable Hermite interpolants, *Math Comput.* 73 (2004), 1913–1935.

[10] R.Q. Jia, and Q.T. Jiang, Approximation power of refinable vectors of functions, in: *Wavelet Analysis and Applications*, AMS/IP Stud. Adv. Math., Vol. 25, Amer. Math. Soc., Providence, RI, 2002, pp. 155–178.

[11] R.Q. Jia and Q.T. Jiang, Spectral analysis of transition operators and its applications to smoothness analysis of wavelets, *SIAM J. Matrix Anal. Appl.* 24 (2003) 1071–1109.

[12] C. Loop, Smooth Subdivision Surfaces Based on Triangles, Master's thesis, University of Utah, Salt Lake City, 1987.

[13] J. Peters and U. Reif, The simplest subdivision scheme for smoothing polyhedra, *ACM Trans. Graphics* 16 (1997), 34–73.

[14] J. Peters and U. Reif, Analysis of algorithms generalizing B-spline subdivision, *SIAM J. Numer. Anal.* 35 (1998), 728–748.

[15] U. Reif, A unified approach to subdivision algorithms near extraordinary vertices, *Comput. Aided Geom. Design* 21 (1995), 153–174.

[16] U. Reif and J. Peters, Structural analysis of subdivision surfaces–a summary, in *Topics in Multivariate Approximation and Interpolation*, K. Jetter et al. (Eds.), 2005.

[17] G. Umlauf, Analyzing the characteristic map of triangular subdivision schemes, *Constr. Approx.* 16 (2000), 145–155.

[18] J. Warren and H. Weimer, *Subdivision Methods For Geometric Gesign: A Constructive Approach*, Morgan Kaufmann Publ., San Francisco, 2002.

[19] D. Zorin, *Stationary Subdivision and Multiresolution Surface Representations*, PhD thesis, California Institute of Technology, Pasadena, 1998.

[20] D. Zorin, A method for analysis of C^1-continuity of subdivision surfaces, *SIAM J. Numer. Anal.* 37 (2000), 1677–1708.

[21] D. Zorin and P. Schröder, A. DeRose, L. Kobbelt, A. Levin, and W. Sweldens, *Subdivision for Modeling and Animation*, SIGGRAPH 2000 Course Notes.

[22] D. Zorin, P. Schröder, and W. Sweldens, Interpolating subdivision for meshes with arbitrary topology, *SIGGRAPH 96*, 1996, pp. 189–192.